# Circuit Modeling, Simulation, and Experimental Validation of a 100-kW Polyphase Wireless Power Transfer System for EV Applications

Omer Onar, Emrullah Aydin, Ahmet Aktas, Mostak Mohammad, Subho Mukherjee, Jon Wilkins, Larry Seiber, and Cliff White
Energy Science and Technology Directorate, Oak Ridge National Laboratory, Oak Ridge, TN
E-mails: onaroc@ornl.gov, aydine@ornl.gov, aktasa@ornl.gov, mohammadm@ornl.gov, mukherjees@ornl.gov, wilkinsjp@ornl.gov, seiberle@ornl.gov, and whitecp@ornl.gov

***Abstract*—Polyphase wireless power transfer (WPT) systems can achieve much higher surface power densities (kW/m$^2$) and specific power levels (kW/kg) compared to the conventional circular single phase WPT systems. Therefore, polyphase WPT systems can reduce the size, weight, volume, and cost of the WPT systems and can simplify the electric vehicle integration with less demand for space. This study presents the high-performance and compact 100-kW WPT development using polyphase electromagnetic coupling coils with rotating magnetic fields.**

***Keywords—Electric Vehicle, Polyphase WPT, Rotating Magnetic Fields, Wireless Power Transfer***

## I. Introduction

Polyphase WPT system can be an enabling technology to achieve high-power levels for wireless charging systems with reasonable size and volume, even suitable for light-duty passenger vehicles. Currently, Society of Automotive Engineers (SAE) J2954 Standard is limited to 11-kW power level with receiver coil size of 420-by-420 mm [1] which is possibly the maximum size that can be integrated into light duty passenger vehicles. At the same time, there are efforts to standardize higher power levels (i.e., 22-, 50-, and 75-kW power levels) as the automotive Original Equipment Manufacturers (OEMs) and customers demand higher power levels. Achieving higher power levels in smaller sizes necessitates advanced coil geometries and designs, offering substantially higher power densities that the conventional single-phase circular/square geometries cannot offer. However, most of the existing WPT systems are predominantly single-phase configurations [2]-[9]. While the adoption of the Silicon Carbide (SiC)-based power devices in WPT systems have facilitated higher power and higher frequency operation, single-phase architectures remain constrained in their maximum power capabilities. These limitations are primarily dictated by the size and mass of the primary and secondary coils, which restrict scalability.



Several notable high-power single-phase WPT developments illustrate these constraints. For instance, a 20-kW wireless charging system designed for the Toyota RAV4 EV [10] achieved a surface pSower density of 31.25 kW/m² with approximately 95 % dc-to-dc efficiency. Similarly, a benchtop demonstration of a 100-kW system [11], [12] demonstrated an impressive surface power density of ~200 kW/m², exceeding 97 % dc-to-dc efficiency, albeit with a substantial coil weight of around 50 kg. Other significant advancements include a modular 65-kW Inductive Power Transfer (IPT) design featuring 600 mm × 600 mm transmitter and receiver pads, yielding a power density of 180 kW/m² [8]. Additionally, the development of 50-kW power electronics-integrated circular and Double-D (DD)-type coil configurations achieved a surface power density of 160 kW/m², with both coil types maintaining the same power level and dimensions [13].

These advancements clearly indicate that current coupler geometries and designs have reached their practical limits in terms of size and mass. To push beyond these constraints, more advanced and innovative designs must be explored to enhance power density, efficiency, and scalability in next-generation WPT systems that are polyphase designs [14]-[22]. This study presents the design and development of a 100-kW polyphase wireless power transfer system with a 750-mm diameter transmitter coil and a 375-mm diameter receiver coil along with their power electronic converters. MATLAB/Simulink circuit simulation results are provided for the LCC-LCC tuned primary and secondary sides, along with the experimental results closely matching the 100-kW polyphase WPT simulation results.

## II. System Description

The proposed system is composed of an open-ended winding inverter on the primary side, LCC-LCC resonant tuning network, primary and secondary (transmitter and receiver) coils, an open-ended rectifier on the vehicle side, and the load (battery pack) at the output of the system. Compared to the conventional three-phase architectures utilizing three half-bridges, open-ended winding design uses two half-bridges or three full-bridges, driving each phase with a dedicated full-bridge inverter with the main advantage of reducing the output phase current by half while doubling the effective output voltage at the inverter output. In this system, each phase winding is powered by an H-bridge inverter, with each inverter phase-shifted by 120° to generate a rotating magnetic field.

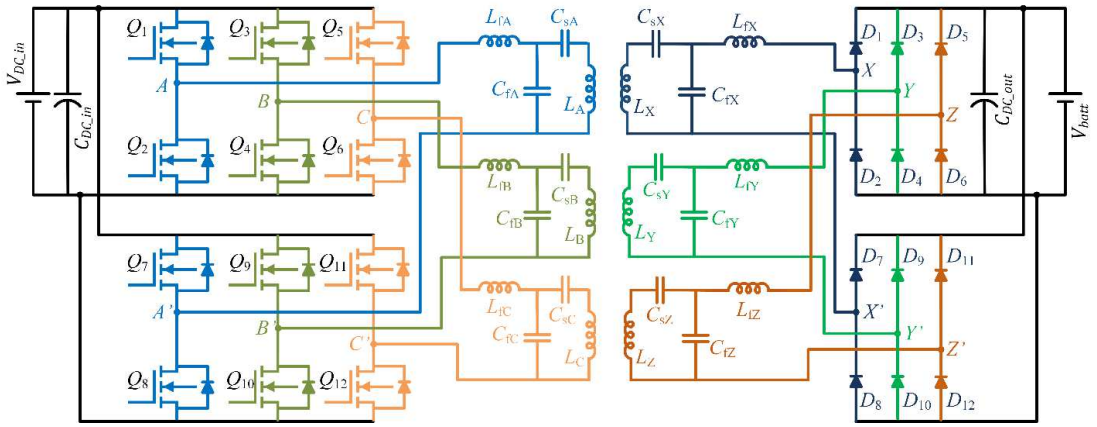


Fig. 1. Polyphase wireless power transfer system design with open-ended winding inverter and rectifier.

This configuration enhances power capability compared to a conventional three-phase inverter with either a delta (Δ) or star (Y) connected load. Both the primary and secondary side couplers utilize LCC resonant tuning network, following the methodology outlined in [14] and [20] for determining component values. The primary-side LCC tuning ensures a constant current behavior that is independent of load and coupling conditions at the resonant frequency. Meanwhile, the secondary-side resonant tuning network facilitates voltage and current conversion between the coils and the rectifier input feeding the load or battery. As illustrated in Figure 1, the primary side consists of three-phase windings labeled *A*, *B*, and *C*, while the secondary side features corresponding three-phase windings labeled *X*, *Y*, and *Z*.

In this three-phase six winding WPT design, each winding has a cross coupling (mutual inductance) with each other. Therefore, a 6-by-6 inductance matrix can be used to describe the self and mutual inductances as shown in (1).

$$L=\begin{bmatrix} L_A & M_{AB} & M_{AC} & M_{AX} & M_{AY} & M_{AZ} \\ M_{BA} & L_B & M_{BC} & M_{BX} & M_{BY} & M_{BZ} \\ M_{CA} & M_{CB} & L_C & M_{CX} & M_{CY} & M_{CZ} \\ M_{XA} & M_{XB} & M_{XC} & L_X & M_{XY} & M_{XZ} \\ M_{YA} & M_{YB} & M_{YC} & M_{YX} & L_Y & M_{YZ} \\ M_{ZA} & M_{ZB} & M_{ZC} & M_{ZX} & M_{ZY} & L_Z \end{bmatrix} \quad (1)$$

Due to the non-zero interphase mutual inductances, the polyphase WPT system requires using an effective equivalent inductance for each phase for resonant tuning network design. As an example, the phase-*A* equivalent inductance for the primary-side and the phase-*X* equivalent inductance for the secondary-side can be expressed by:

$$L_A^{'}=L_A - M_{AB} + M_{BC} - M_{AC} \quad (2)$$

$$L_X^{'}=L_X - M_{XY} + M_{YZ} - M_{XZ} \quad (3)$$

Therefore, the resonant tuning inductors and capacitors for primary-side can be computed by (4) and for the secondary-side by (5), respectively.

$$\omega L_A^{'} - \frac{1}{\omega C_{sA}} = \frac{1}{\omega C_{fA}} = \omega L_{fA} \quad (4)$$

$$\omega L_X^{'} - \frac{1}{\omega C_{sX}} = \frac{1}{\omega C_{fAX}} = \omega L_{fX} \quad (5)$$

## III. System Parameters and Simulation Results

The inductance matrix of the proposed polyphase wireless power transfer system is provided in (6) and the resistance matrix is given in (7) while the resonant tuning components are listed in Table 1. The transmitter and receiver coil rendered drawings are provided in Fig. 2.

$$L=\begin{bmatrix} 17.56 & -4.65 & -4.60 & 2.15 & -1.87 & -0.64 \\ -4.65 & 17.12 & -4.65 & -0.65 & 2.44 & -1.79 \\ -4.60 & -4.65 & 17.65 & -1.86 & -0.76 & 2.33 \\ 2.15 & -0.65 & -1.86 & 14.79 & -4.12 & -4.01 \\ -1.87 & 2.44 & -0.76 & -4.12 & 14.87 & -4.22 \\ -0.64 & -1.79 & 2.33 & -4.01 & -4.22 & 15.02 \end{bmatrix} \mu H \quad (6)$$

$$R=\begin{bmatrix} 15 & 0 & 0 & 0 & 0 & 0 \\ 0 & 15 & 0 & 0 & 0 & 0 \\ 0 & 0 & 15 & 0 & 0 & 0 \\ 0 & 0 & 0 & 22 & 0 & 0 \\ 0 & 0 & 0 & 0 & 22 & 0 \\ 0 & 0 & 0 & 0 & 0 & 22 \end{bmatrix} m\Omega \quad (7)$$

In this design, a load voltage of 560 V was considered to represent a vehicle with 800 V battery platform with an almost fully depleted (state-of-charge < 10 %) battery. At this voltage and power level, the equivalent resistive load would be:

$$R=\frac{560^2}{100000}=3.1\ \Omega \quad (8)$$

TABLE I. THE PARAMETERS OF THE WPT SYSTEM

| Parameter | Value | Unit |
|---|---|---|
| $L_{fA}=L_{fB}=L_{fC}$ | 5.97 | µH |
| $C_{fA}=C_{fB}=C_{fC}$ | 0.65 | µF |
| $C_{sA}=C_{sB}=C_{sC}$ | 0.24 | µF |
| $L_{fX}=L_{fY}=L_{fZ}$ | 10.56 | µH |
| $C_{fX}=C_{fY}=C_{fZ}$ | 0.38 | µF |
| $C_{sX}=C_{sY}=C_{sZ}$ | 0.422 | µF |
| $R_{load}$ | 3.1 | Ω |
| $V_{dc\_in}$ | 570 | V |
| $I_{dc\_in}$ | 183.9 | A |
| $V_{dc\_out}$ | 557.7 | V |
| $I_{dc\_out}$ | 179.9 | A |
| TX diameter | 750 | mm |
| RX diameter | 375 | mm |
| TX wire structure | 3×4 AWG wires / phase, 3 turns | |
| RX wire structure | 1×2 AWG wires / phase, 3 turns | |

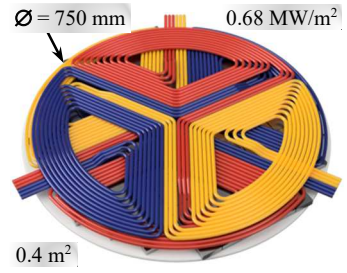


(a)

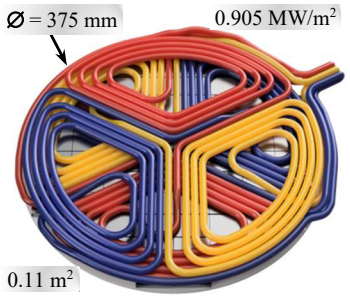


(b)

Fig. 2. The design of the transmitter (a) and receiver (b) side polyphase coils.

For the input dc voltage, the boost power factor rectification of 400 V three-phase system was considered, that would provide about 570 V dc input at the primary-side inverter. Under these conditions, the inverter output three-phase voltages and currents are provided in Fig. 3 (a) while Fig. 3 (b) shows the vehicle-side rectifier input voltages and currents.

Here, the currents are negative when the inverter is turned on, indicating zero turn-on losses in the inverter with the Zero-Voltage-Switching (ZVS) operation while there is a small turn off current when the inverter is turned off for each phase with minimal turn off switching losses. On the other hand, rectifier is inherently running at unity power factor as the rectifier currents flow only when the voltage exists to forward bias the rectifier diodes

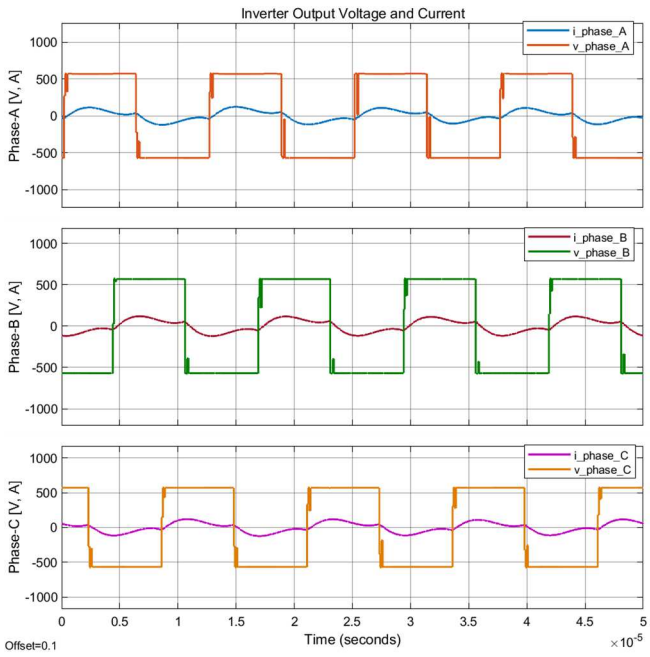


(a)

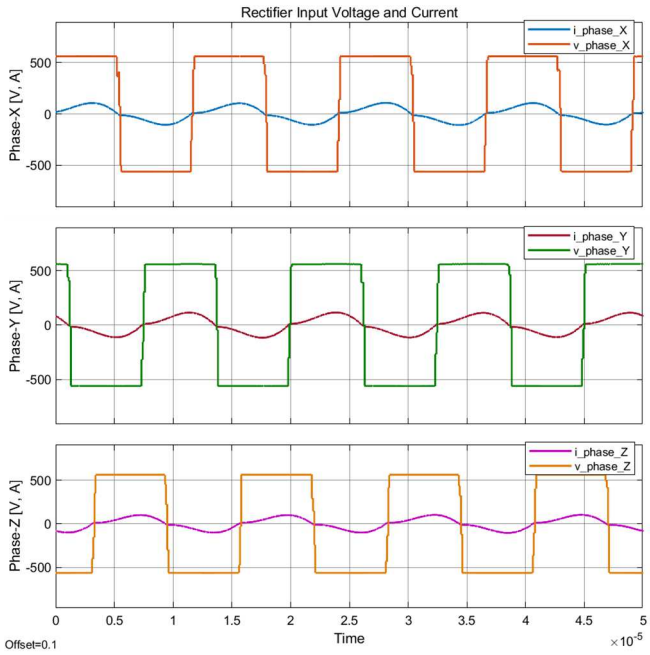


(b)

Fig. 3. Simulation results of the polyphase WPT system inverter output voltages and currents on transmitter side (a) and rectifier input voltages and currents on the receiver side (b).

At the same time, transmitter coil currents are presented in Fig. 4 (a) while the receiver coil currents are presented in Fig. 4 (b). On the transmitter, each phase carries about 166 Amps Root Mean Square (RMS) current. With 3 wires in parallel per phase, each wire on the transmitter carries 55.33 Amps RMS approximately. On the receiver side, each phase carries about 97 Amps RMS at these conditions at 100 kW power transfer to the load.

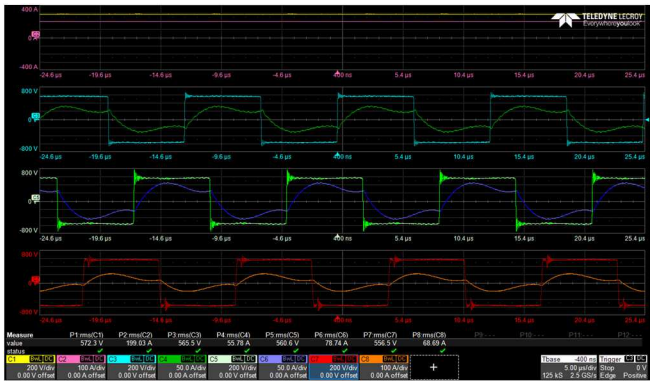

Fig. 4. Experimental results of the polyphase WPT system inverter output voltages and currents on transmitter side.

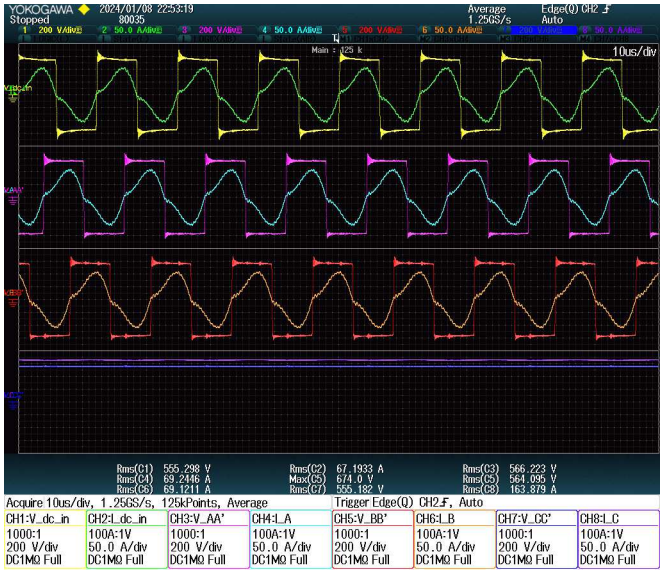

Fig. 5. Experimental results of the polyphase WPT system rectifier input voltages and currents on the receiver side.

TABLE II. EXPERIMENTAL RESULTS OF THE POLYPHASE WPT SYSTEM

| Primary side | Values | Secondary side | Values |
|---|---|---|---|
| $V_{dc\_in}$ | 572.3 V | $V_{dc\_out}$ | 555.1 V |
| $I_{dc\_in}$ | 199.03 A | $I_{dc\_out}$ | 163.87 A |
| $V_{tXA}$ | 565.5 V | $V_{rXA}$ | 555.2 V |
| $I_{tXA}$ | 55.78 A | $I_{rXA}$ | 67.19 A |
| $V_{tXB}$ | 560.6 V | $V_{rXB}$ | 566.2 V |
| $I_{tXB}$ | 78.74 A | $I_{rXB}$ | 69.24 A |
| $V_{tXC}$ | 556.5 V | $V_{rXC}$ | 564.0 V |
| $I_{tXC}$ | 68.69 A | $I_{rXC}$ | 69.12 A |

Simulation results show that inverter output currents are approximately 72 Amps RMS while the rectifier input currents are about 70 Amps RMS. According to the dc input voltages and currents and dc output voltages and currents shown in Table I., the input power is recorded 104.823 kW and output power is recorded 100.33 kW which corresponds to a dc-to-dc efficiency of $\eta_{dc\text{-}to\text{-}dc} = 95.71$ %.

It should be noted that in the simulation model, 5 mΩ internal resistance was assumed for all the resonant tuning components, with an additional 1 mΩ resistance at the inverter and rectifier input and output interconnections while the on-resistance ($R_{ds\_on}$) of 3.25 mΩ for inverter MOSFETs and 2 V of forward voltage drop ($V_{fwd}$) for rectifier and 2 mΩ of contact resistance for each diode were considered.

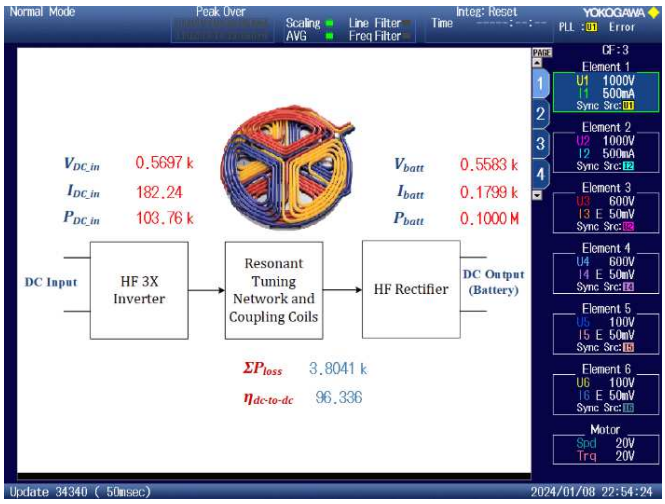


Fig. 6. The dc-to-dc efficiency of the polyphase WPT system in experimental studies at 100 kW output power.

In the experimental results, the current and voltage results at the output of the inverter on the transmitter side are given in Fig. 4, and the current and voltages at the rectifier input on the receiver side are given in Fig. 5. In the experimental studies, 100 kW of power was transferred to the receiver side. The dc-to-dc efficiency of the WPT system was measured as 96.336 % and is given in Fig. 6. Under this power, the dc bus voltage at the WPT system input ($V_{dc\_in}$) was measured as 572.3 V and the voltage at the output ($V_{dc\_out}$) was measured as 555.1 V. Table II shows the dc bus and phase current voltage values for the dc transmitter and receiver sides.

This study presents a 100-kW polyphase WPT system design, modeling, and simulations for EV charging applications. The proposed system's power electronics architecture uses open-ended winding inverter and rectifier for the highest flexibility in the power electronic. The experimental test photograph is given in Fig. 7.

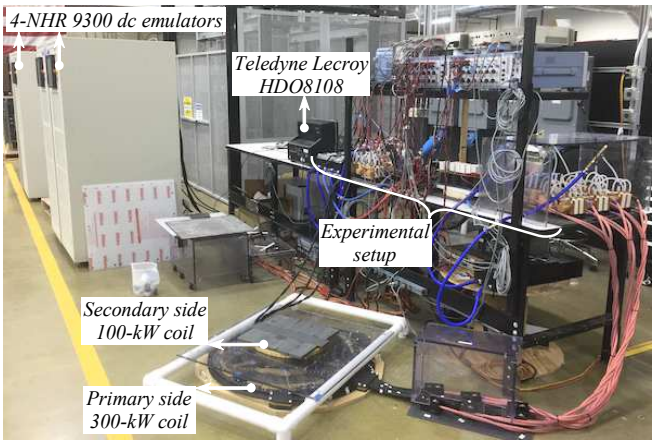


Fig. 7. Experimental test setup of the polyphase WPT system.

## IV. Conclusions

This study presents a 100-kW polyphase WPT system design, modeling, simulations, and experimental validation for an EV charging application. The proposed system's power electronics architecture uses open-ended winding inverter and rectifier for the highest flexibility in the power electronic converters while offering simplicity in scaling up the power capability of the converters. Simulation results indicate 95.7 % and experimental results measure 96.336 % efficiency at 100 kW power transfer level, considering all the realistic parasitic and losses in the system components including power electronics, resonant tuning networks, and the coils.

## Acknowledgment

This research used the resources available at the Power Electronics and Electric Machinery (PEEM) Laboratory at the National Transportation Research Center (NTRC), a U.S. DOE user facility operated by Oak Ridge National Laboratory (ORNL). The authors would like to thank Lee Slezak and Fernando Salcedo (Vehicle Technologies Office, US DOE) and John Jason Conley (National Energy Technology Laboratory) for funding this work and for their continuous support and guidance.

## References

[1] SAE J2954 Standard, "Wireless Power Transfer for Light-Duty Plug-in/Electric Vehicles and Alignment Methodology," 08/2024, available online: https://www.sae.org/standards/content/j2954_202408/

[2] Brusa Inductive Charging System ICS115 Operation Manual for Installation-Operation-Maintenance, available online: https://fcc.report/FCC-ID/2AK2AICS115/4193329.pdf

[3] P. Schumann, T. Diekhans, O. Blum, U. Brenner, and A. Henkel, "Compact 7 kW inductive charging system with circular coil design," in Proc., International Electric Drives Production Conference (EDPC), pp. 1-5, September 2015, Nuremberg, Germany.

[4] H. Feng, R. Tavakoli, O. C. Onar, and Z. Pantic, "Advances in high-power wireless charging systems: Overview and design considerations," IEEE Transactions on Transportation Electrification, vol. 6, no. 3, pp. 886-919, September 2020.

[5] R. Bosshard and J. W. Kolar, "Inductive power transfer for electric vehicle charging: Technical challenges and tradeoffs," *IEEE Power Electronics Magazine*, vol. 3, no. 3, pp. 22-30, Sept. 2016.

[6] M. Suzuki, K. Ogawa, F. Moritsuka, T. Shijo, H. Ishihara, Y. Kanekiyo, K. Ogura, S. Obayashi, M. Ishida, "Design method for low radiated emission of 85 kHz band 44 kW rapid charger for electric bus," in Proc., IEEE Applied Power Electronics Conference and Exposition (APEC), pp. 3695-3701, March 2017, Tampa, FL.

[7] R. Bosshard and J. W. Kolar, "Multi-Objective Optimization of 50 kW/85 kHz IPT System for Public Transport," IEEE Journal of Emerging and Selected Topics in Power Electronics, vol. 4, no. 4, pp. 1370 1382, December 2016.

[8] J. M. Miller, A. W. Daga, F. J. McMahon, P. C. Schrafel, B. Cohen, A. W. Calabro, "A Closely Coupled and Scalable High-Power Modular Inductive Charging System for Vehicles," IEEE Journal of Emerging and Selected Topics in Power Electronics, vol. 10, no. 3, pp. 3259-3272, June 2022.

[9] Idaho National Laboratory Advanced Vehicle Testing Activity, DC Charger Fact Sheet: WAVE 250kW Wireless Charger on 40' BYD Bus, available online: https://cet.inl.gov/ArticleDocuments/WAVE_250kW_FactSheet.pdf

[10] O. C. Onar, M. Chinthavali, S. L. Campbell, L. E. Seiber, C. P. White, and and V. P. Galigekere, "Modeling, simulation, and experimental verification of a 20-kW series-series wireless power transfer system for a Toyota RAV4 electric vehicle," in *Proc., IEEE Transportation Electrification Conference and Expo (ITEC)*, pp. 874-880, June 2018, Long Beach, CA.

[11] J. Pries, V. P. Galigekere, O. C. Onar, G. -J. Su, R. Wiles, L. Seiber, J. Wilkins, S. Anwar, and S. Zou, "Coil power density optimization and trade-off study for a 100kW electric vehicle IPT wireless charging system," in *Proc., IEEE Energy Conversion Congress and Exposition (ECCE)*, pp. 1196-1201, September 2018, Portland, OR.

[12] V. P. Galigekere, J. Pries, O. C. Onar, G. -J. Su, S. Anwar, R. Wiles, L. Seiber, and J. Wilkins, "Design and implementation of an optimized 100 kW stationary wireless charging system for EV battery recharging," in *Proc., IEEE Energy Conversion Congress and Exposition (ECCE)*, pp. 3587-3592, September 2018, Portland, OR.

[13] R. Bosshard, U. Iruretagoyena, and J. W. Kolar, "Comprehensive evaluation of rectangular and double-D coil geometry for 50 kW/85 kHz IPT system," *IEEE Journal of Emerging and Selected Topics in Power Electronics*, vol. 4, no. 4, pp. 1406-1415, December 2016.

[14] J. Pries, V. P. N. Galigekere, O. C. Onar, and G. -J. Su, "A 50-kW Three-Phase Wireless Power Transfer System Using Bipolar Windings and Series Resonant Networks for Rotating Magnetic Fields," *IEEE Transactions on Power Electronics*, vol. 35, no. 5, pp. 4500-4517, May 2020.

[15] A. Aktas, O. C. Onar, E. Asa, M. Mohammad, B. Ozpineci, and L. M. Tolbert, "Sensitivity Analysis of a Polyphase Wireless Power Transfer System Under Off-Nominal Conditions," *IEEE Transactions on Transportation Electrification*, vol. 10, no. 3, pp. 6690-6706, Sept. 2024.

[16] E. Asa, O. Onar, M. Mohammad, V. P. Galigekere, G. -J. Su, and B. Ozpineci, "Overview of High-Power Wireless Charging Systems and Analysis of Polyphase Wireless Charging System Phase Winding and Resonant Tuning Network Connection Configurations," *IEEE Transactions on Transportation Electrification (early access)*, doi: 10.1109/TTE.2024.3514841.

[17] R. Zeng, O. C. Onar, M. Mohammad, G. Su, E. Asa, and V. P. Galigekere, "Modeling and Analysis of a Polyphase Wireless Power Transfer System for EV Charging Applications," in *Proc., IEEE Applied Power Electronics Conference and Exposition (APEC)*, Houston, TX, USA, 2022, pp. 1885-1890.

[18] M. Mohammad, O. C. Onar, V. P. Galigekere, G. -J. Su, and J. Wilkins, "Thermal Design and Optimization of High- Power Wireless Charging System," in *Proc., IEEE Applied Power Electronics Conference and Exposition (APEC)*, Houston, TX, USA, 2022, pp. 480-485.

[19] M. Mohammad, O. C. Onar, J. L. Pries, V. P. Galigekere, G. -J. Su, and J. Wilkins, "Thermal Analysis of a 50 kW Three-Phase Wireless Charging System," in *Proc., IEEE Transportation Electrification Conference & Expo (ITEC)*, Chicago, IL, June 2021.

[20] M. Mohammad, J. L. Pries, O. C. Onar, V. P. Galigekere, G. -J. Su and J. Wilkins, "Three-Phase LCC-LCC Compensated 50-kW Wireless Charging System with Non-Zero Interphase Coupling," in Proc., *IEEE Applied Power Electronics Conference and Exposition (APEC)*, Phoenix, AZ, June 2021, pp. 456-462.

[21] M. Mohammad, J. L. Pries, O. C. Onar, V. P. Galigekere and G. -J. Su, "Shield Design for 50 kW Three-Phase Wireless Charging System," in Proc., *IEEE Energy Conversion Congress and Exposition (ECCE)*, Detroit, MI, October 2020, pp. 842-849.

[22] E. Aydin, H. Barua, A. Aktas, M. Mohammad, O. C. Onar and B. Ozpineci, "Thermal Analysis of a 100 kW Polyphase Wireless Power Transfer System," in *Proc., IEEE Applied Power Electronics Conference and Exposition (APEC)*, Long Beach, CA, February 2024, pp. 1927-1931.